A Large-Deformation Theory for Thermally-Actuated Shape-Memory Polymers and its Application

Proceedings of the ASME 2010 International Mechanical Engineering Congress & Exposition
IMECE2010
November 12-18, 2010, Vancouver, British Columbia, Canada

IMECE2010-37383

A LARGE-DEFORMATION THEORY FOR THERMALLY-ACTUATED SHAPE-MEMORY POLYMERS AND ITS APPLICATION

Shawn A. Chester, Vikas Srivastava, Claudio V. Di Leo, and Lallit Anand
Solid Mechanics and Materials Laboratory,
Department of Mechanical Engineering,
Massachusetts Institute of Technology,
Cambridge, Massachusetts 02139, USA

INTRODUCTION

The most common shape-memory polymers are those in which the shape-recovery is *thermally-induced*. A body made from such a material may be subjected to large deformations at an elevated temperature above its glass transition temperature ϑ_g. Cooling the deformed body to a temperature below ϑ_g under active kinematical constraints fixes the deformed shape of the body. The original shape of the body may be recovered if the material is heated back to a temperature above ϑ_g without the kinematical constraints. This phenomenon is known as the *shape-memory effect*. If the shape recovery is partially constrained, the material exerts a recovery force and the phenomenon is known as *constrained-recovery*.

As reviewed by [1], one of the first widespread applications of shape-memory polymers was as heat-shrinkable tubes. Such rudimentary early applications did not necessitate a detailed understanding or modeling of the thermomechanical behavior of these materials. However, in recent years shape-memory polymers are beginning to be used for critical biomedical applications, microsystems, re-writable media for data storage, and self-deployable space structures. In order to develop a robust simulation-based capability for the design of devices for such critical applications, one requires an underlying accurate thermo-mechanically-coupled constitutive theory and an attendant validated numerical implementation of the theory.

In the past few years several efforts at experimental characterization of the thermo-mechanical stress-strain response of a wide variety of shape-memory polymers have been published in the literature [1, 2] to name a few. Significant modeling efforts have also been published [2, 3] to name a few. However, at this point in time, a thermo-mechanically-coupled large-deformation constitutive theory for modeling the response of thermally-actuated shape-memory polymers is not widely agreed upon — the field is still in its infancy. The purpose of this manuscript is to present results from of our own recent [4], and ongoing research in this area.

Specifically, with the aim of developing a thermo-mechanically-coupled large-deformation constitutive theory and a numerical simulation capability for modeling the response of thermally-actuated shape-memory polymers, we have (i) conducted large strain compression experiments on a representative shape-memory polymer to strains of approximately unity at strain rates of 10^{-3} s^{-1} and 10^{-1} s^{-1}, and at temperatures ranging from room temperature to approximately 30 C above the glass transition temperature of the polymer; (ii) formulated a thermo-mechanically-coupled large deformation constitutive theory; (iii) calibrated the material parameters appearing in the theory using the stress-strain data from the compression experiments; (iv) numerically implemented the theory by writing a user-material subroutine for a widely-used finite element program; and (v) conducted representative experiments to validate the predictive capability of our theory and its numerical implementation in complex three-dimensional geometries. By comparing the numerically-predicted response in these validation simulations against measurements from corresponding experiments, we show that our theory is capable of reasonably accu-

rately reproducing the experimental results. Also, as a demonstration of the robustness of the three-dimensional numerical capability, we show results from a simulation of the shape-recovery response of a stent made from the polymer when it is inserted in an artery modeled as a compliant elastomeric tube.

Furthermore, as is well known, when the shape-memory polymer recovers from its temporary shape it returns stored energy and can serve as a thermally-activated actuator. Due to the low rubbery modulus of the polymer above the glass transition temperature, its actuation force is limited and the material is thus restricted form numerous applications where "high" actuation forces are required. To combat the problem of low actuation force of shape-memory polymers, we have synthesized reinforced shape-memory polymer composites using superelastic nitinol wires. Specifically with these reinforced composites we have (i) conducted thermo-mechanical three-point bend experiments on samples with and without nitinol wires. In these experiments the deformation is constrained so as to measure the actuation force; (ii) numerically simulated the thermo-mechanical response of the shape-memory polymer composite in the aforementioned condition of constrained recovery using the simulation capability developed. The numerical predictions are in good agreement with the experimental results of constrained-recovery of the reinforced shape-memory composites.

EXPERIMENTAL CHARACTERIZATION OF A SHAPE-MEMORY POLYMER

As a representative thermally-actuated shape-memory polymer we chose to characterize the mechanical response of a chemically-crosslinked thermoset polymer recently studied by [5]. Following a procedure described by these authors, the shape-memory polymer was synthesized via photopolymerization (UV curing) of the monomer tert-butyl acrylate (tBA) with the crosslinking agent poly(ethylene glycol) dimethacrylate (PEGDMA), in the following specific composition: tBA 90% by weight (mol. weight: 128 g/mol) with PEGDM 10% by weight (mol. weight: 550 g/mol).

The chemicals were mixed in a glass beaker for 2 minutes, and the mixed liquid solution was then degassed in a vacuum chamber for 10 minutes. The degassed mixture was then injected between two glass sheets that were separated with spacers. A UV-Lamp was used to photopolymerize the solution at an intensity of $\sim 30\,\mathrm{mW/cm^2}$ for 10 minutes. Finally, the polymer was heat-treated at 90 C for 1 hour to complete the polymerization reaction.

This polymer is chosen for study because the shape-memory actuation temperature for this polymer is close to that of body-temperature — the *nominal* glass transition temperature for this polymer is $\vartheta_g \approx 37\,\mathrm{C}$ [6].

We have conducted a set of simple compression experiments on this polymer. The cylindrical specimens were 6.3 mm diameter and 3.15 mm tall. The compression experiments were conducted at true-strain rates of $10^{-3}\,\mathrm{s}^{-1}$ and $10^{-1}\,\mathrm{s}^{-1}$ at 22 C, 30 C, 40 C, 50 C, and 65 C, up to true strain-levels of $\approx 100\%$. Figure 1 shows a few representative true stress-strain curves at a constant true strain rate of $0.1\,\mathrm{s}^{-1}$ and various temperatures. The polymer exhibits two distinctly different responses at temperatures below and above ϑ_g:

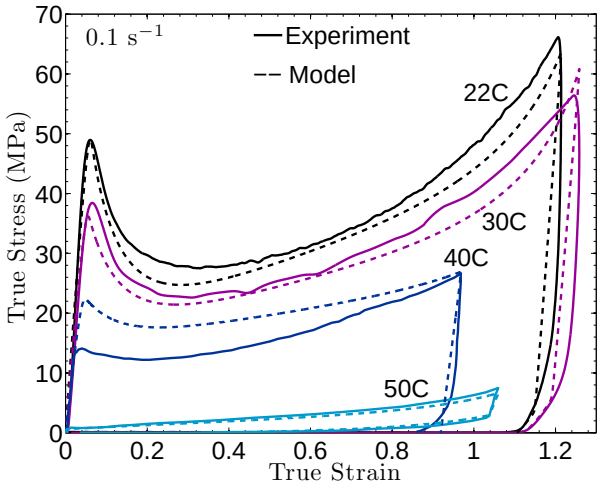

Figure 1. Compressive true stress-strain response of the shape-memory polymer at a constant true strain rate of $0.1\,\mathrm{s}^{-1}$ and various temperatures as indicated. Solid lines are experimental data, and the dashed lines are the model fit.

- The stress-strain curves at 22 C and 30 C are below ϑ_g. At these temperatures the polymer exhibits a strain-rate and temperature-dependent response typical of a "glassy-polymer". That is, a well-defined yield-peak, followed by strain-softening, and eventual rapid strain-hardening at large strains. Upon unloading after compression to a strain level of $\approx 100\%$, about 5% of the strain is recovered and the remainder is left as a "permanent-set" (as long as the temperature is held constant).
- The stress-strain curve at 50 C is above ϑ_g. At these temperatures the material exhibits a "hysteretic-rubber"-like response. That is, the initial stiffness of the material drops dramatically from its value below ϑ_g, the yield-peak disappears, and upon unloading there is essentially no permanent set. However, there is significant hysteresis in the stress-strain response which is significantly rate- and temperature-dependent.

Of particular interest is the stress-strain curve at 40 C, a temperature which is in the vicinity of the *nominal* glass transition temperature of $\vartheta_g \approx 37\,\mathrm{C}$. At the lower strain rate of $10^{-3}\,\mathrm{s}^{-1}$ (not shown in the Figure) the material responds like a "hysteretic-

rubber", while at the higher strain rate of $10^{-1}\,s^{-1}$ the material responds like a "glassy-polymer." Thus, in accordance with the well-known result from frequency-dependent dynamic-mechanical-tests on amorphous polymers, this result shows that the "glass transition temperature" ϑ_g is *not a constant* for a material — it increases as the strain rate increases.

SUMMARY OF THE CONSTITUTIVE THEORY

In this section we present a brief summary of the constitutive theory given in [4]. Although no real material is composed of springs and dashpots, as a visual aid, Figure 2 shows a schematic "spring-dashpot" rheological representation of our three micromechanism model.

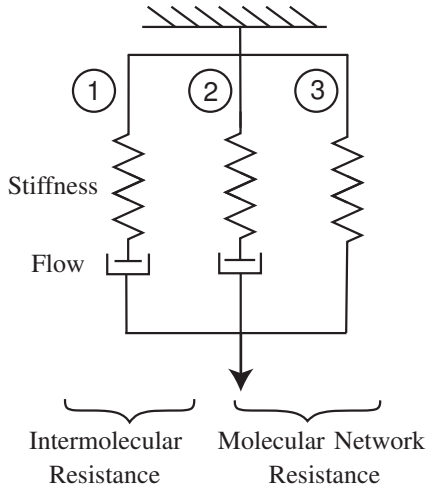

Figure 2. A schematic "spring-dashpot" representation of the model.

These three micromechanisms are intended to represent the following underlying physical phenomena: **Micromechanism (1)**: The nonlinear spring represents an "elastic" resistance due to intermolecular energetic bond-stretching. The dashpot represents thermally-activated plastic flow due to "inelastic mechanisms," such as chain-segment rotation and relative slippage of the polymer chains between neighboring cross-linkage points. **Micromechanisms (2,3)**: In addition to the chemical crosslinks which are present throughout the temperature range of interest in thermoset polymers, at temperatures below ϑ_g we expect that the polymer also exhibits a significant amount of mechanical-crosslinking. We conceptually distinguish molecular chains between mechanical-crosslinks and molecular chains between chemical-crosslinks by introducing two micromechanisms, 2 and 3, respectively. The nonlinear springs in these two mechanisms represent resistances due to changes in the free energy upon stretching of the molecular chains between the crosslinks. The mechanical-crosslinks are expected to disintegrate when the temperature is increased through ϑ_g; the dashpot in micromechanism 2 represents thermally-activated plastic flow resulting from such a phenomenon. The micromechanism 3 represents chemically-crosslinked backbone of the thermoset polymer in which the crosslinks do not slip.

The material parameters in the constitutive theory were calibrated by fitting the model to the simple compression experiments described previously. As a representative example, Figure 1 shows a comparison between the experiments and the model. For full details of the constitutive theory, including that for general amorphous polymers, the reader is referred to [4, 7–9].

VALIDATION EXPERIMENTS AND SIMULATIONS

In order to validate the predictive capabilities of our constitutive theory and its numerical implementation, in this section we show the results of two thermo-mechanical experiments that we have performed on the tBA/PEGDMA shape-memory polymer, and compare the results of macroscopic measurements from these experiments against results from corresponding numerical simulations. The validation experiments considered below are:

(i) Measurement of the displacement-versus-time response of a planar specimen of tBA/PEGDMA in the shape of a diamond-shaped lattice which was subjected to the following thermo-mechanical history: the specimen was compressed between two platens at temperature above ϑ_g of the material, the compression platens were then held fixed while the specimen was cooled to a temperature below ϑ_g. The constraint of the platens was then removed, and the specimen was heated to a temperature above ϑ_g and allowed to freely recover its shape. We call an experiment of this type an unconstrained-recovery or a free-recovery experiment.

(ii) Measurement of the force-versus-time response of a ring-shaped specimen of tBA/PEGDMA which was subjected to the following thermo-mechanical history: the specimen was heated to a temperature above ϑ_g of the material, the ring was then compressed into an oval shape, the compression grips were then held fixed while the specimen was first cooled to a temperature below ϑ_g, and then heated back to its initial temperature above ϑ_g. We call an experiment of this type a constrained-recovery experiment.

Free-recovery

The flat diamond-lattice-shaped specimen, Figure 3a, was 50 mm wide, 35 mm tall, and 3 mm thick. Each diamond-shaped cut-out was a square with 6.5 mm sides with a 1 mm fillet-radius at the corners; the width of the ligaments forming the lattice was 2.16 mm.

The specimen was subjected to the following thermo-mechanical history: (i) it was compressed between two platens at

60 C at a relative platen velocity of 0.02 mm s^{-1}, and the height of the specimen was reduced from 35 mm to 20.5 mm — this resulted in an increase in its width from 50 mm to 59.5 mm; (ii) the platens were held in place and the specimen was cooled to 21 C — the deformed shape is shown in Figure 3b; (iii) the compression platens were then removed and the specimen was heated to 58 C. The dimensional changes in the specimen during this unconstrained-recovery phase were measured using a video-extensometer. The experimentally-measured stretches (L/L_0) in the 1- and 2-directions as functions of temperature and time during the unconstrained heating phase of the experiment are shown in Figure 4 and Figure 5, respectively.

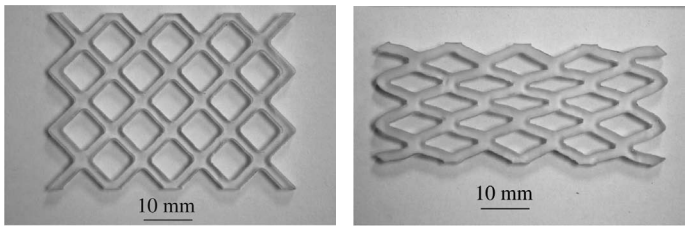

(a) (b)

Figure 3. Diamond-shaped-lattice specimen: (a) Undeformed specimen. (b) Deformed specimen in its "temporary shape" at room temperature – deformed at 60 C, constrained cooling to 21 C, and constraints removed.

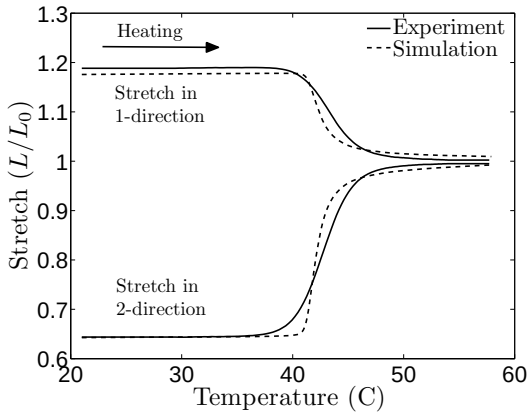

Figure 4. The solid lines show the experimentally measured stretch-temperature curves in the 1- and 2-direction during the unconstrained heating phase of the experiment. The dashed lines are the corresponding numerically predicted results.

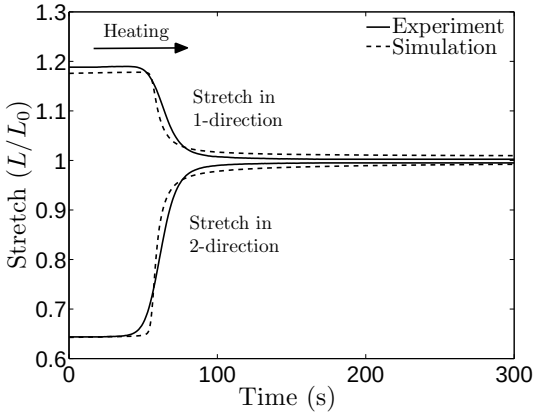

Figure 5. The solid lines show the experimentally measured stretch-temperature curves in the 1- and 2-direction during the unconstrained heating phase of the experiment. The dashed lines are the corresponding numerically predicted results.

For the finite element simulation of this experiment we make use of the symmetry of the geometry and only mesh one-eighth of the geometry, using 1962 ABAQUS-C3D8HT thermo-mechanically-coupled elements. Our numerical simulation included all the steps described above for the thermo-mechanical history, including the initial hot-deformation, cooling, and finally the unconstrained shape-recovery with the applied temperature change. Figure 4 and Figure 5 compare the numerically-predicted and experimentally-measured stretches in the 1- and 2-directions versus temperature and time, respectively, during the unconstrained heating phase of the experiment. The numerically-predicted results are in good agreement with experimental measurements.

Constrained-recovery

The flat specimen, 3 mm thick, was ring-shaped with two extension arms which were used for gripping the specimen. The ring portion of the specimen had an outer diameter of 11.9 mm and an inner diameter of 6.3 mm, while the extension arms were each 12.7 mm long and 4.1 mm wide. The experimental set-up with the tBA/PEGDMA specimen mounted in place within the furnace of the EnduraTEC testing machine is shown in Figure 6. The top and the bottom flat surfaces of the extension arms were rested against the base of the grips, and the vertical sides were securely tightened in the grips.

The specimen was subjected to the following thermo-mechanical history: (i) it was heated to 58 C and gripped; (ii) the bottom grip was fixed in place while the top grip was moved downwards at a velocity 0.01 mm s^{-1} for a total displacement of 2.5 mm to deform the ring; (iii) the grips were then held fixed in their positions and the specimen was first cooled to 32 C and then

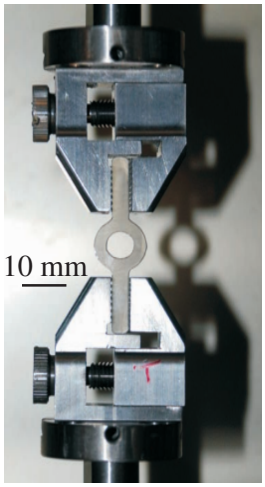

Figure 6. Experimental set-up for the thermo-mechanical constrained-recovery experiment on a ring-shaped specimen of tBA/PEGDMA.

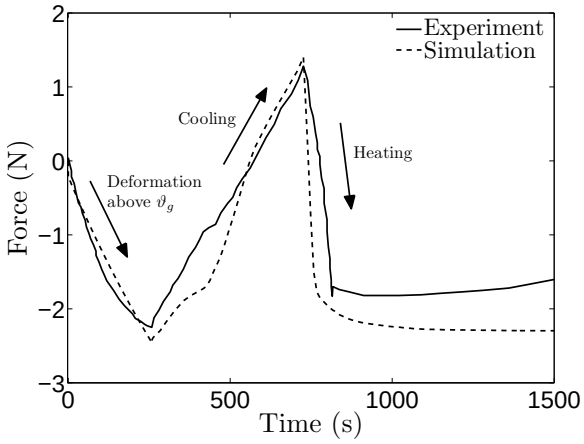

Figure 7. The solid line shows the experimentally measured force-time curve for the constrained-recovery experiment. The corresponding numerically predicted response is shown as a dashed line.

heated back to 58 C.

For the finite element simulation of this constrained-recovery experiment we make use of the symmetry of the geometry, and only mesh one-eighth of the geometry using 537 ABAQUS-C3D8HT thermo-mechanically-coupled elements. Figure 7 compares the experimentally-measured and the numerically-predicted force-versus-time curves. The measurements from the experiment show that a compressive force was generated during the deformation at 58 C. Subsequently, under the fixed-grip conditions, upon cooling to 32 C the compressive force gradually reduces and transitions to a state of tension; and finally, upon heating back to 58 C, the reaction force transitions back to a compressive state. As shown in Figure 7, the simulation is able to reasonably accurately predict the force-versus-time response for the constrained-recovery experiment.

APPLICATIONS

Vascular Stent

As a numerical example, we consider a vascular stent application. The stent was subjected to the following thermo-mechanical history: (i) it was radially compressed above ϑ_g at 60 C to reduce its outer diameter to 4.7 mm from 8.0 mm; (ii) cooled under kinematical constraints to 22 C at a rate of 0.1 C s^{-1} to fix its deformed shape; (iii) the constraints were removed; (iv) following which it was inserted into an arterial tube; and (v) was heated back to 60 C at a rate of 0.1 C s^{-1} to allow the stent to attempt to recover its initial shape under the constraints imposed by the artery. Due to the symmetry of the problem in our simulation we considered only one-eighth of the stent geometry, which was modeled using 1077 ABAQUS-C3D8HT thermo-mechanically-coupled elements. To apply the initial deformation above ϑ_g, all of the nodes at the outer diameter were given an inward radial displacement. The finite element mesh for the artery consisted of 1500 ABAQUS-C3D8H elements: 2 elements through the thickness, 50 elements along the length, and 15 elements around the one-quarter circumference. The atery is modeled as an incompressible Neo-Hookean material with a shear modulus of 33.33 kPa. Contact between the stent and artery was modeled as frictionless. Figure 8a shows the initial undeformed stent, while Figure 8b shows the deformed stent after radial compression at 60 C. Figure 8c shows snapshots of the stent inside the artery during shape-recovery at 22°C, 42°C, and 60°C.

Composite Beams

In order to increase the actuation force produced by a shape memory polymer when recovering an initial deformation under kinematic constrains, we synthesized a composite composed of super-elastic nitinol wires suspended in a shape memory polymer matrix. The manufacturing process and chemical composition of the polymer is identical to that presented earlier, with the sole distinction that the degassed polymer mixture was injected between two glass slides separated by a sandwich of aluminum spacers and nitinol wires. The casting structure suspended the nitinol wires inside the liquid polymer mixture during the UV curing process and was removed after the curing was completed. The nitinol wires used were 0.5 mm in diameter and composed of 56 % Nickel and 44 % Titanium. Beams being 2.5 mm thick, 50.8 mm long, and 20.3 mm wide were manufactured with one nitinol wire and no nitinol wires in the polymer matrix. A beam with the same dimensions and width of 31.8 mm was manufactured with two nitinol wires suspended in the polymer matrix. Figure 9a shows a sample beam with two nitinol wires.

The actuation force was measured through thermo-

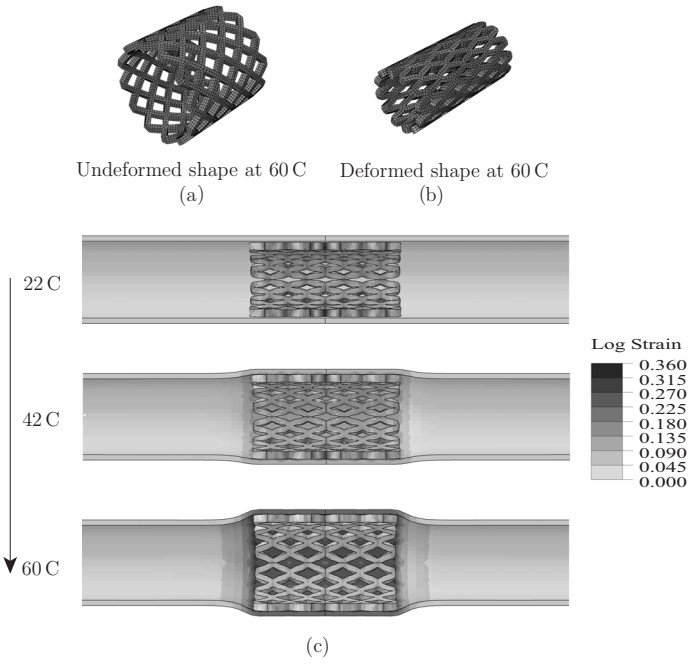

Figure 8. (a) Undeformed original mesh. (b) Deformed stent. (c) Shape-recovery of the stent inside the artery with temperature.

mechanical three-point bend testing. The specimen was subjected to the following thermo-mechanical history: (i) it was heated to 65 C for 30 minutes and then bent by displacing the top fixture 10 mm. (ii) The fixture was then held fixed and the specimen was allowed to cool to 25 C for 30 minutes. (iii) The specimen was reheated to a temperature of 65 C while the fixture was held constant and the load on the fixture was measured. It is important to note that the load measurement was only taken during the re-heating of the specimen. Figure 9b shows the experimental three-point bend set up mounted in place within the furnace of the EnduraTEC testing machine prior to re-heating the specimen.

For the finite element simulation of this constrained-recovery experiment we make use of the symmetry of the geometry, and only mesh one-quarter of the geometry using 1802, 3602, and 5002 ABAQUS-C3D8HT thermo-mechanically coupled elements for the no-nitinol, one-nitinol, and two-nitinol wire simulations, respectively. The constitutive model used for the nitinol wires is the ABAQUS built-in implicit user subroutine for nitinol with the default material parameters.

Figure 10 compares the experimentally-measured and the numerically-predicted force-versus-time curves. The measurements from the experiment show that the introduction of just a single nitinol wire increases the actuation force from ≈ 0.4 N to ≈ 2 N, a five fold increase. With two nitinol wires the actuation force is increased to ≈ 4 N, a ten fold increase. As shown in Figure 10, the simulation is able to reasonably accurately predict the

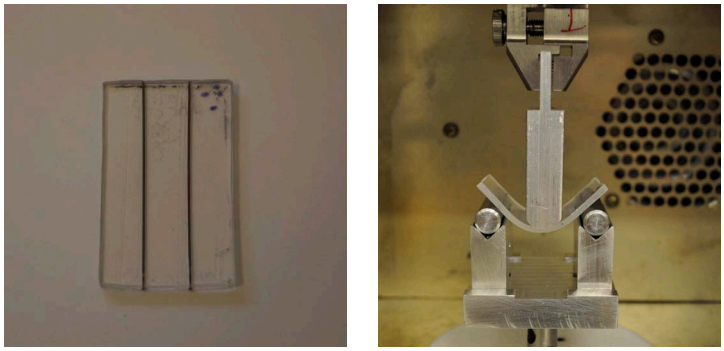

Figure 9. (a) Nitinol-reinforced shape-memory polymer composite beam with two nitinol wires suspended in the polymer matrix. (b) Experimental set-up for thermo-mechanical constrained three-point bend testing of nitinol-reinforced shape-memory polymer beams.

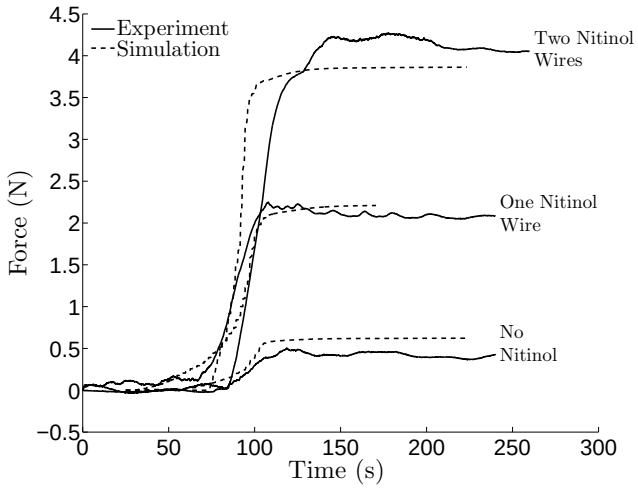

Figure 10. The solid lines show the experimentally measured actuation force behavior for the constrained-recovery three-point bend experiment. The corresponding numerically predicted responses are shown as dashed lines.

force-versus-time response of the nitinol reinforced shape memory polymer composites. The simulation capabilities developed here are thus capable of being used as a tool in the design of thermally-activated actuators based on nitinol-reinforced shape memory polymers composites. For full details of the manufacturing, testing, and simulation of nitinol-reinforced shape memory polymers, the reader is referred to [10]

CONCLUDING REMARKS

We have reviewed our recently developed thermo-mechanically-coupled large-deformation constitutive theory and

a numerical simulation capability for modeling the response of thermally-actuated shape-memory polymers given in [4]. The theory and methodology developed in this study offers the potential for the development of a robust simulation-based capability for the design of devices made from shape-memory polymers for a variety of applications.

Furthermore, we have synthesized nitinol-reinforced shape memory polymers to increase the actuation force of shape-memory polymers. We have shown, that in the case of a flat beam under three-point bending, the actuation force can be increased ten fold by the use of nitinol wires as reinforcing members of the polymer matrix. The composite beams illustrate one possible application of shape-memory polymers as thermally activated actuators.

REFERENCES

[1] Gall, K., Yakacki, C., Liu, Y., Shandas, R., Willet, N., and Anseth, K., 2005. "Thermomechanics of the shape-memory effect in polymers for biomedical applications". *Journal of Biomedical Materials Research Part A*, **73A**, pp. 339–348.

[2] Qi, H., Nguyen, T., Castro, F., Yakacki, C., and Shandas, R., 2008. "Finite deformation thermo-mechanical behavior of thermally induced shape-memory polymers". *Journal of the Mechhanics and Physics of Solids*, **56**, pp. 1730–1751.

[3] Nguyen, T., Qi, H., , Castro, F., and Long, K., 2008. "A thermoviscoelastic model for amorphous shape-memory polymers: Incorporating structural and stress relaxation". *Journal of the Mechhanics and Physics of Solids*, **56**, pp. 2792–2814.

[4] Srivastava, V., Chester, S., and Anand, L., 2010. "Thermally-actuated shape-memory polymers: experiments, theory, and numerical simulations". *Journal of the Mechanics and Physics of Solids*, **58**, pp. 1100–1124.

[5] Yakacki, C., Lanning, R. S. C., Rech, B., Eckstein, A., and Gall, K., 2007. "Unconstrained recovery characterization of shape-memory polymer networks for cardiovascular applications". *Biomaterials*, **28**, pp. 2255–2263.

[6] Safranski, D., and Gall, K., 2008. "Effect of chemical structure and crosslinking density on the thermo-mechanical properties and toughness of (meth)acrylate shape-memory polymer networks". *Polymer*, **49**, pp. 4446–4455.

[7] Anand, L., Ames, N., Srivastava, V., and Chester, S., 2009. "A thermo-mechanically-coupled theory for large deformations of amorphous polymers. part i: formulation". *International Journal of Plasticity*, **25**, pp. 1474–1494.

[8] Ames, N., Srivastava, V., Chester, S., and Anand, L., 2009. "A thermo-mechanically-coupled theory for large deformations of amorphous polymers. part ii: applications". *International Journal of Plasticity*, **25**, pp. 1495–1539.

[9] Srivastava, V., Chester, S., and Anand, L., 2010. "A thermo-mechanically-coupled large deformation theory for amorhpous polymers in a temperature range which spans their glass transition". *International Journal of Plasticity*, **26**, pp. 1138–1182.

[10] DiLeo, C. V., 2010. Nitinol-reinforced shape-memory polymers. BS thesis, Massachusetts Institute of Technology, Cambridge, MA.